

Experimental evaluation of emission models from a thermal evaporation source

S Cronjé, W D Roos and R E Kroon

Department of Physics, University of the Free State, Bloemfontein, South Africa

Email: KroonRE@ufs.ac.za

Abstract. Thermal evaporation is a well-known phenomenon used to produce metallic thin films for many industrial and research applications. Generally the focus is not on the evaporation rate, but the deposition rate which can be measured using a quartz crystal microbalance (QCM). In this study the interest is in the evaporation process, for which well-known models such as the Hertz-Knudsen equation exist but are not always accurate. A novel approach was developed to use the deposition rate on a QCM to study the evaporation flux from a surface. This required a model for the angular distribution of evaporating atoms in order to link the measured deposition rate to the evaporation rate. The literature generally assumes a point source with a $\cos^n \varphi$ angular dependence and $n = 0, 1, 2$ etc corresponding to isotropic emission, cosine emission associated with Knudsen effusion cells and more directed emissions, respectively. To measure low evaporation rates the model considers evaporation from a surface placed so close to the QCM that the assumption of a point source is questionable. Since a treatment of the evaporation rate from an extended source was not found in literature, a model was developed by treating the extended surface as many point sources and integrating numerically. The fraction of evaporated atoms incident on the QCM for point and extended circular sources for $n = 0, 1, 2$ and 3 are compared. The results also predict how the deposition rate should change with the distance between source and QCM. This is compared to data measured for the evaporation of antimony from a custom designed resistance heater in an ultrahigh vacuum environment to determine the most suitable emission model.

1. Introduction

The production of thin films is of great importance in research and industrial applications as diverse as the growth of conducting layers in microelectronics [1] to the coating of the mirrors of optical telescopes [2]. Various physical vapour deposition (PVD) techniques exist where the process of evaporation is the source of the deposited material [3]. Generally the focus is on the deposition rate, since these techniques are end-product driven. The fundamentals of evaporation can, however, be investigated using the equipment employed in these techniques. These fundamentals are of importance where the surface loss of samples due to evaporation takes place during sample surface characterization.

In this study the deposition rate of pure Sb, as measured by a quartz crystal microbalance (QCM) commonly employed in PVD techniques was used to relate the amount of deposited material measured to the actual amount of material that evaporated from the evaporation source. This required a model for the angular distribution of evaporating atoms in order to link the measured deposition rate to the evaporation rate.

2. Theory

2.1. Point source

Deposition of thin films involves consideration of both the characteristics of the evaporation source and the orientation and placement of the substrate upon which the evaporated atoms or molecules impinge. In addition, only a fraction of the evaporant leaving the sample surface impedes on the quartz crystal. Evaporation from a point source is the simplest of situations to model and the details are well-known [4]. Consider a point on a surface from which particles are evaporating. The particles may leave with equal probability at any angle (isotropic), or they may follow the so-called cosine law often used for Knudsen cells. The particles may even be directed more strongly upwards from a deep narrow crucible. In general one may assume that the particles leave a point on the surface with an angular dependence $\cos^n \varphi$ where φ is the angle relative to the surface normal. Figure 1 illustrates this.

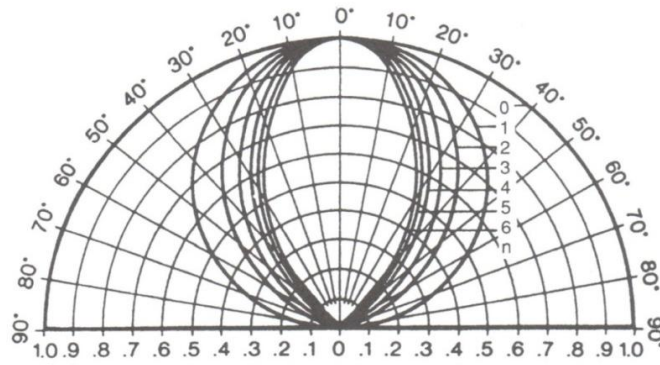


Figure 1. Calculated lobe-shaped vapour clouds using the cosine law $\cos^n \varphi$ where φ is the angle relative to the surface normal at that point: $n = 0$ corresponds to the isotropic case, while $n = 1$ is a simple model for a surface or Knudsen cell, and $n = 2$ or higher correspond to more directed anisotropic sources applicable for a narrow deep evaporation crucibles [4].

In a case where n is large, the vapour flux is highly directed. Physically n is related to the evaporation crucible geometry and scales directly with the ratio of the melt depth below the top of the crucible to the melt surface area [4]. More specifically in the case of this study n is related to the sample holder geometry.

If the particle path makes an incidence angle θ relative to the normal of the collecting surface a distance r away, then the mass per unit area deposited on the substrate is $\frac{M_e(n+1) \cos^n \varphi \cos \theta}{2\pi r^2}$ where M_e is the total evaporated mass [4] and hence the fraction of particles collected on an area A_s is given by

$$\int_{A_s} \frac{(n+1) \cos^n \varphi}{2\pi} \frac{\cos \theta}{r^2} dA_s. \quad (1)$$

Equation 1 can be applied to a flat collecting surface (see figure 2a) lying a distance h directly above and parallel to the emission point. Then the angles φ and θ are equal, with $\cos \varphi = \cos \theta = h/r$. If the collecting area is a disk of radius r_s directly above the emission point then the expression becomes

$$\int_{l=0}^{r_s} \frac{(n+1) \cos^{n+1} \varphi}{2\pi} \frac{\varphi}{r^2} (2\pi l dl) \quad (2)$$

and noting that $r = \sqrt{h^2 + l^2}$, integration gives the fraction of collected particles as

$$1 - [1/(1 + (r_s/h)^2)]^{\frac{(n+1)}{2}}. \quad (3)$$

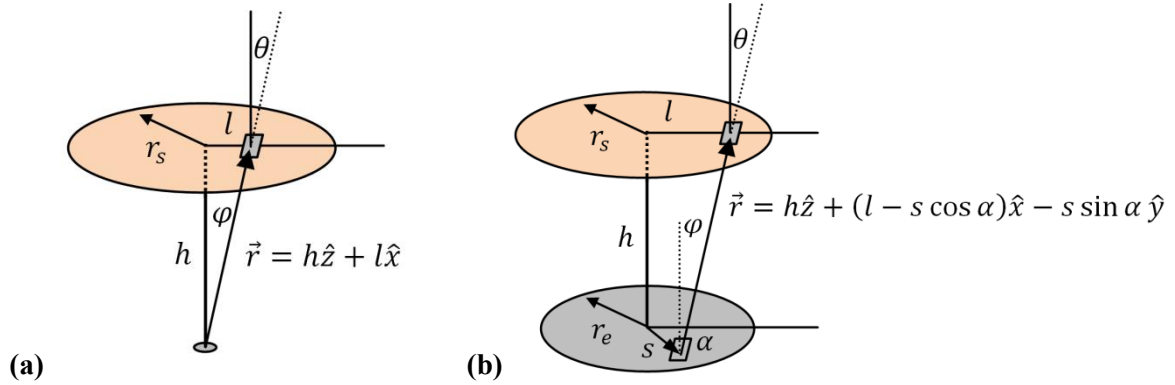


Figure 2. (a) Particles evaporating from a point on a surface and being collected on a disk of radius r_s that is a distance h directly above the point source. (b) Particles evaporating from an extended disk surface of radius r_e and being collected on a disk of radius r_s that is a distance h directly above the extended source.

2.2. Extended source

Consider now evaporation not from a point source, but rather from a distributed region or surface area. This leads to a situation as shown in figure 2b. Taking the total evaporating region as a disk of radius r_e directly below and parallel to the collecting disk, equation 2 needs to be modified by considering how the value of $(\cos^{n+1} \varphi)/r^2$ varies as the emission point $(x, y) = (s \cos \alpha, s \sin \alpha)$ moves over the surface of the emitting disk. This results in a new model for evaporation from an extended surface given by

$$\int_{l=0}^{r_s} \frac{(n+1)}{2\pi} \left[\frac{1}{\pi r_e^2} \iint_{A_e} \frac{\cos^{n+1} \varphi}{r^2} dA_e \right] (2\pi l dl). \quad (4)$$

In this case $r = \sqrt{h^2 + (l - s \cos \alpha)^2 + (s \sin \alpha)^2}$, so equation 4 can be rewritten as

$$\frac{(n+1)h^{n+1}}{\pi r_e^2} \int_{l=0}^{r_s} \int_{\alpha=0}^{2\pi} \int_{s=0}^{r_e} \frac{sl}{[h^2 + (l - s \cos \alpha)^2 + (s \sin \alpha)^2]^{\frac{(n+3)}{2}}} ds d\alpha dl \quad (5)$$

which may be evaluated numerically.

3. Experimental setup and procedure

A sample stage manipulator and an Inficon XTC/3s QCM were fitted to an Auger Electron Spectroscopy (AES) system. This allowed the user to reposition a sample mounted on a resistance heater from a position in front of the electron gun/analyser to a position underneath the QCM, as illustrated in figure 3. Not only can the sample surface thus be analysed before an evaporation experiment is performed, but also the surface can also be sputter cleaned from any contaminants that might influence the evaporation rate.

A 99.999% pure Sb disk was used as an evaporation sample. The AES system was evacuated to a base pressure of 3×10^{-8} torr, and after heating the sample to 673 K the average evaporation rate as measured by the QCM over a time interval of 1 min was recorded for various separation distances between the samples surface and the QCM, which was set accurately using a micrometer and varied between 0.5 cm and 3.0 cm for the measurements.

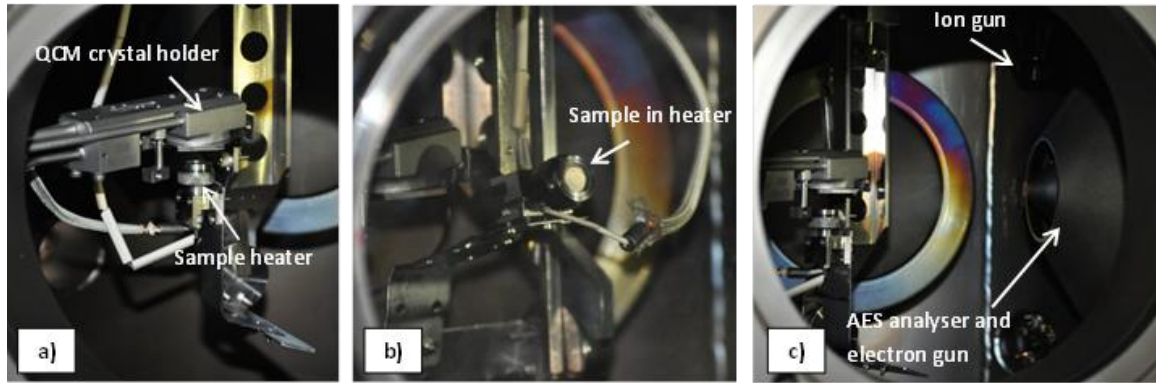


Figure 3. The different parts of the modifications made and how they relate in terms of position to each other: (a) The QCM crystal holder with the sample heater positioned under it for an evaporation run. (b) The sample being moved by means of a manipulator and rotated towards the AES analyzer shown in (c).

4. Results and discussion

The fractions of collected particles were theoretically calculated for the experimental conditions ($r_e = 0.395$ cm and $r_s = 0.4125$ cm) using equation 3 for a point source and equation 5 for an extended source for various angular distributions (n) and separation distances (h). For the numerical evaluation of equation 5, the Matlab function ‘triplequad’ was used. This data is given in table 1.

Table 1. Percentage of emitted particles from an evaporation source with $\cos^n \varphi$ point angular distribution that is incident on a circular capturing surface of radius $r_s = 0.4125$ cm at a distance h directly above it.

h (cm)	Point source				Extended source ($r_e = 0.395$ cm)			
	$n = 0$	$n = 1$	$n = 2$	$n = 3$	$n = 0$	$n = 1$	$n = 2$	$n = 3$
0.5	22.86%	40.50%	54.10%	64.60%	18.95%	32.37%	42.12%	49.40%
1	7.56%	14.54%	21.00%	26.97%	6.94%	13.03%	18.41%	23.17%
1.5	3.58%	7.03%	10.36%	13.57%	3.42%	6.63%	9.64%	12.47%
2	2.06%	4.08%	6.06%	7.99%	2.01%	3.94%	5.80%	7.59%
2.5	1.33%	2.65%	3.95%	5.23%	1.31%	2.59%	3.84%	5.05%
3	0.93%	1.86%	2.77%	3.68%	0.92%	1.83%	2.71%	3.59%
3.5	0.69%	1.37%	2.05%	2.72%	0.68%	1.35%	2.02%	2.67%
4	0.53%	1.05%	1.57%	2.09%	0.52%	1.04%	1.56%	2.06%
4.5	0.42%	0.83%	1.25%	1.66%	0.42%	0.83%	1.24%	1.64%
5	0.34%	0.68%	1.01%	1.35%	0.34%	0.67%	1.00%	1.34%

As expected, the collected fractions for an extended source are always smaller than the corresponding value for a point source, although the differences become negligible for larger separations. For both the point source and extended source models, the collected fraction increases with increasing n which corresponds to more directed evaporation.

The experimentally measured deposition rates and the theoretically calculated fractions of collected particles cannot be compared directly. To test which theoretical model best corresponded to the experimental results, all sets of data were normalized relative to a fixed separation distance, namely $h = 3$ cm which was the maximum experimental value used. The relative change in the experimental deposition rate should then be directly comparable to the relative change in the collected fraction of the theoretical models as the separation distance is varied. The comparison is shown in figure 4, where the horizontal axis giving the separation distance is given on a log scale.

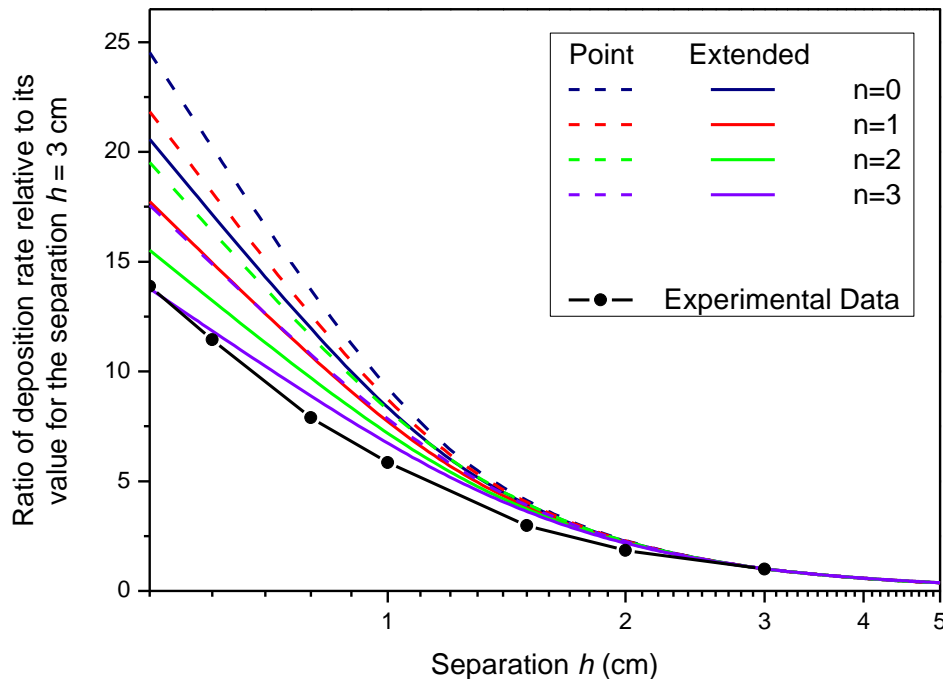


Figure 4. Comparison of the relative experimental deposition rate as a function of separation distance compared to the relative collected fraction using various models.

As the separation decreases, the relative collected fraction based on the theoretical calculations increases faster for the point sources compared to the extended sources for the same n value, because for the extended sources it is more likely for some particles to pass outside the collecting surface. Also, for both the point and extended sources, the relative collected fraction increases faster with decreasing separation distance for the less directed emission distributions (smaller n values). The least increase in relative collection fraction with decreasing separation distance occurs for an extended source of high directionality (large n), and this corresponds best to the experimental observations made for the evaporation of Sb. Although the form of the experimental curve and the theoretical curves do not match very well, it is clear that the experimental data coincides better for the evaporation model from an extended source and for high directionality (n).

5. Conclusion

The results show that assuming the Knudsen model ($n = 1$) for point sources can lead to serious errors when considering evaporation and that the new evaporation model for an extended source and for high directionality (n) provides a better fit to the experimental data in the case of evaporation of antimony from a custom designed resistance heater in an ultrahigh vacuum environment. This evaporation model best fitting the experimental data predicts how the deposition rate should change with the distance between the source and QCM and provides the necessary link of the most suitable emission model which is necessary to study evaporation rates by using measurements of deposition rates.

References

- [1] Cao Z 2011 *Thin Film Growth* (Sawston: Woodhead Publishing Limited)
- [2] Phillips A C, Miller J S, Bolte M, Doprav B, Radovan M and Cowley D 2012 Progress in UCO's search for silver-based telescope mirror coatings, Proc. SPIE 8450 doi:10.1117/12.925502
- [3] Mattox D M 2010 *Handbook of Physical Vapor Deposition (PVD) Processing* 2nd Edition (Amsterdam: Elsevier)
- [4] Ohring M 2002 *Materials Science of Thin Films* 2nd Edition (San Diego: Academic Press)